THE JOURNAL OF BIOLOGICAL CHEMISTRY
Vol. 273, No. 1, Issue of January 2, pp. 177–185, 1998
Printed in U.S.A.

The Dynamic Properties of the M121H Azurin Metal Site as Studied by NMR of the Paramagnetic Cu(II) and Co(II) Metalloderivatives*

(Received for publication, July 30, 1997, and in revised form, October 13, 1997)

Jesús Salgado‡, Sandra J. Kroes‡, Axel Berg‡, José M. Moratal§¶, and Gerard W. Canters‡¶

From the ‡Leiden Institute of Chemistry, University of Leiden, P.O. Box 9502, 2300 RA Leiden, The Netherlands and §Department of Inorganic Chemistry, University of Valencia, Dr. Moliner 50, 46100 Burjassot (Valencia), Spain

The M121H azurin mutant in solution presents various species in equilibrium that can be detected and studied by ^{1}H NMR of the Cu(II) and Co(II) paramagnetic metalloderivatives. In both cases up to three species are observed in slow exchange, the proportions of which are different for the two metalloderivatives. Above pH 5 the major species displays a tetrahedral coordination in which the His^{121} can be observed as a coordinated residue. Its metal site corresponds to a new type of site that is defined as a type 1.5 site. The second and third species resemble the wild type (type 1) azurin and, above pH 4.5, they are present only at a low concentration. At low pH a protonation process increases the proportion of both type 1 species at the expense of the type 1.5 species. This process, characterized by a pK_a = 4.3, is assigned to the protonation of His^{121}. At high pH the NMR spectrum of the Co(II)-M121H azurin experiences an additional transition, which is not observed in the case of the Cu(II) protein. The dynamic properties of the M121H metal site appear to be related to changes in the coordination geometry and the strength of the axial interaction between the N$^{\delta 1}$ (His^{121}) and the metal.

An important challenge in protein engineering is the creation or modification of metal sites in proteins (1, 2). Properties that one might wish to manipulate range from metal binding strength and metal site stability to redox potential, catalytic activity, and substrate specificity. One way to meet this task is the creation of novel metal binding sites in proteins or protein domains that in their native state have no such site (3–7). This approach depends heavily on computer-assisted modeling and automated searches for appropriate attachment sites of side chains that can act as metal ligands. The side chains must be able to attain an orientation that is favorable for strong metal binding while at the same time leaving sufficient room for possible substrate binding. The method is demanding and success is not within easy reach, but when successful the result can be spectacular (3–7).

A second approach makes use of natural metalloproteins and modifies existing metal sites by applying changes in the first and second coordination shell of the metal (1, 8). The advantage of this approach is that it is relatively easy to implement and that the native site provides a solid background against which the properties of the newly created site can be evaluated. Prime examples of proteins for which the second approach has been successful are the heme proteins (9) and copper-containing proteins such as superoxide dismutase (10) and the blue copper proteins (11, 12).

The work described here focuses on the blue copper protein azurin from *Pseudomonas aeruginosa*. In azurin the metal in the active site is immobilized by three strong ligands (the nitrogen donors His^{46} and His^{117}, and the sulfur donor Cys^{112}) and a fourth weaker axial ligand (the sulfur donor Met^{121}) (13). The carbonyl oxygen of Gly^{45} provides for an additional axial interaction (13). The spectroscopic properties of the metal site are dominated by the copper-sulfur (Cys^{112}) interaction (14). In the native protein this interaction is responsible, among others, for two sulfur-copper charge transfer transitions in the optical absorption spectrum, a weak one around 400 nm and a strong one around 600 nm, a pattern that is characteristic of a (distorted) tetrahedral "type 1" site (14). By modifying the side chain ligands an optical spectrum can be obtained in which the intensity of the two bands is reversed (10, 15). This spectroscopic change corresponds with a change in the copper site geometry from (distorted) tetrahedral to square planar, a configuration that is typical of a "type 2" copper site (15).

Among the ligand mutations that have been explored so far there is one type of modification that leads to a site of which the characteristics have not been properly understood until now (16, 17). When Met^{121} is replaced by an ionizable ligand such as lysine, glutamic acid, or histidine the spectroscopic properties of the site become dependent upon pH and temperature (16, 17). For instance, in the optical spectrum the intensity of the band at 400 nm increases at high pH at the expense of the 600-nm band (17). Changes with pH can also be observed by nuclear magnetic relaxation dispersion (18) and in the RR,[1] EPR (17), and perturbed angular correlation spectra (19).

Since the optical properties seem to be intermediate between those of a type 1 and a type 2 site, the new site has been called "type 1.5" (17). Although structural information on this site has been lacking until now it was thought that the coordination geometry might correspond with a tetrahedral ligand configuration in which the copper has moved out of the plane of its three canonical strong ligands in the direction of the axial ligand at position 121 (17). Preliminary data from x-ray diffraction studies support this idea.[2] However, this provides no clue as to the origin of the pH effects. The changes with pH appear more complicated than what might be expected on the basis of a simple two-state equilibrium, and until now it has not been

* This work was supported in part by the Netherlands Foundation for Chemical Research (S.O.N.) with financial aid from the Netherlands Organization for Scientific Research (N.W.O.) and by the Spanish "Dirección General de Investigación Científica y Técnica" (D.G.I.C.Y.T., PB 94-0989). The costs of publication of this article were defrayed in part by the payment of page charges. This article must therefore be hereby marked "*advertisement*" in accordance with 18 U.S.C. Section 1734 solely to indicate this fact.

¶ To whom correspondence should be addressed. Tel.: 31-71-5274256; Fax: 31-71-5274349; E-mail: canters@chem.leidenuniv.nl.

[1] The following abbreviations have been used: RR, resonance Raman; EPR, electron paramagnetic resonance; WEFT, water-eliminated Fourier transformation; NOE, nuclear Overhauser effect; NOESY, nuclear Overhauser effect spectroscopy; EXSY, exchange spectroscopy; wt, wild type; pH*, pH meter readings in D_2O samples.

[2] A. Messerschmidt, unpublished observations.

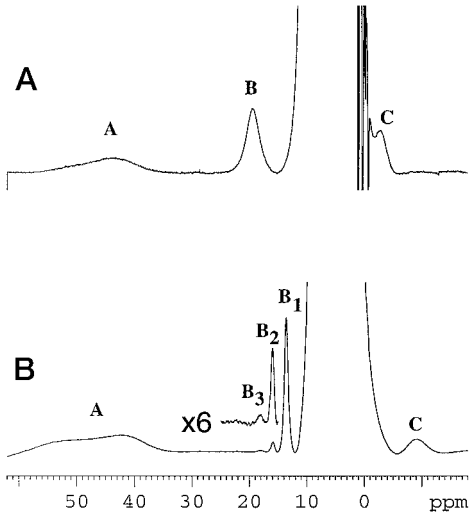

FIG. 1. **600 MHz ^{1}H NMR spectra of Cu(II)-M121H azurin in D_2O (*A*) at pH* 6.0 and 20 °C and Cu(II)-wt azurin (*B*) at pH 5.5 and 32 °C.**

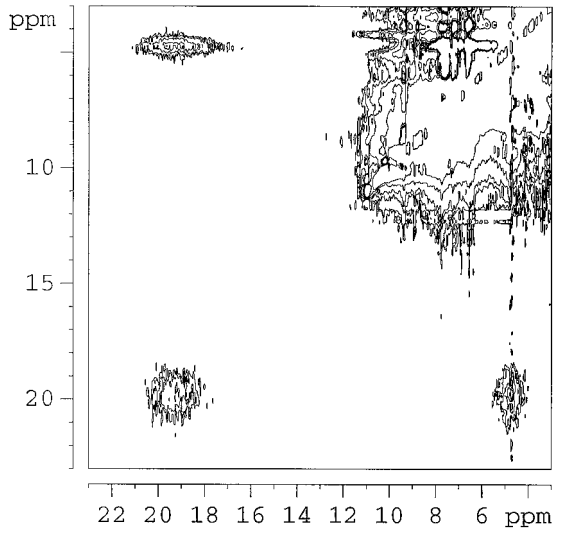

FIG. 2. **600 MHz WEFT-EXSY map of a 50% oxidized sample of wild type *A. denitrificans* azurin in D_2O.** The spectrum has been recorded at pH* 5.5 and 32 °C using a 3-ms mixing time.

possible to unravel the behavior of the site with pH.

Apparently, changing the metal side chain ligands may introduce fluxionality in the metal binding site. Since this may have a strong bearing on the redox properties or the catalytic activity of a metal site in general, it is important for future reference to try and establish the basis of this fluxionality as accurately as possible. Attempts to pinpoint the nature of the changes that a type 1.5 site undergoes with pH, met with little success (17–19). The methods employed were either not sensitive enough to monitor all the species in solution or the time scale of the technique did not match the time scale of the motion within the site. As the Cu(II) form of the protein is by far the most accessible for spectroscopic characterization (as opposed to the Cu(I) form), all efforts have focused on this form of the protein. Unfortunately, the paramagnetism of the active site seemed to preclude the application of high resolution NMR techniques. The recent successful application of "paramagnetic NMR" to the blue copper proteins has made it clear, however, that with special precautions regarding sample preparation and pulse techniques, the active site of paramagnetic blue copper proteins can be studied in detail by NMR (20). These investigations can be complemented with the NMR study of the Co(II) derivatives (21, 22), which exhibit similar dynamic properties but give more extensive NMR information due to their more favorable relaxation properties (23).

Here the details of the dynamic behavior of a type 1.5 site are reported for the case of the M121H variant of azurin from *P. aeruginosa*. It is shown that the equilibrium features of the site, as observed by EPR, paramagnetic NMR (Cu(II), and Co(II) derivatives), RR, and optical techniques, can be analyzed by invoking a three state equilibrium corresponding with three different geometries of the copper site, and that two of these geometries allow the protonation/deprotonation of His^{121}. The results are important in that they illustrate the difficulties encountered in unraveling the type of fluxionality a metal site may become susceptible to, when the native environment of the metal is tampered with. The findings may have important implications for the design of novel or modified metal sites in proteins.

EXPERIMENTAL PROCEDURES

Protein Preparation—Wild-type (wt) and M121H *Alcaligenes denitrificans* azurins were obtained from the expression of the corresponding genes in *Escherichia coli* as reported previously (17, 24). The Co(II) metalloderivative was prepared by the addition of 5 molar equivalents of $CoSO_4$ to the apoprotein solution at room temperature, and the metal uptake was followed by UV-visible spectroscopy (25). Samples for NMR experiments were concentrated by ultrafiltration in Centricon-10 concentration cells (Amicon) up to 4–5 mM.

pH meter readings of D_2O samples have not been corrected for the deuterium isotopic effect, and they are denoted as pH*.

Spectroscopic Measurements and Calculations—^{1}H NMR spectra were recorded on Varian Unity spectrometers operating at 300 or 400 MHz and on a Bruker DMX 600 MHz spectrometer. The super-WEFT pulse sequence (26) was used to detect the fast relaxing signals of the spectrum and to eliminate the solvent H_2O or hydrogen deuterium oxide signal.

EXSY and NOESY experiments were performed in a phase-sensitive mode using the WEFT-NOESY pulse sequence (27) with delays, τ, of 25–50 ms between the 180 ° and 90 ° pulses and with mixing times of 3–10 ms. The spectra were Fourier-transformed using 512 or 1024 data points in both dimensions and square sine-bell weighting functions shifted 60 or 80 °.

T_1 values were calculated by single exponential fitting of the signal intensities observed in an inversion-recovery experiment (23). pK_a values were determined from the area, A, of the ^{1}H NMR signals of spectra recorded at different pH values, by fitting the data to the following equation

$$A = A_{max}/(10^{[pK_a^{ap} - pH]} + 1) \quad \text{(Eq. 1)}$$

where A_{max} is the area of the signal at high pH and pK_a^{ap} stands for the apparent pK_a (see "Discussion"). As noted before (17) the spectral changes with pH and temperature appear reversible in the pH range 3.5–10.5 and in the temperature range 5–55 °C. At pH 3–3.5 (irreversible) denaturation of the protein sets in slowly. Electronic spectra were recorded on a Cary 1 spectrophotometer.

RESULTS

Cu(II)-M121H Azurin

The ^{1}H NMR spectrum of Cu(II)-wt azurin in D_2O is shown in Fig. 1*A*. It is characterized by the presence of very broad resonances between 40 and 60 ppm (**A**), a sharper peak between 10 and 20 ppm (**B**), and an upfield-shifted peak (**C**). In the case of the Cu(II)-wt amicyanin, signals similar to **A**, **B**, and **C** have been assigned to the imidazole δ_2 protons of His^{96} and His^{54}, the α proton of Cys^{93} and the β_1 proton of His^{54}, respectively, by EXSY spectroscopy on a 50% oxidized sample (20). We have detected an exchange peak only for signal **B** (Fig. 2), which connects it to the Cys^{112} C$^{\alpha}$H proton. The high electron self-exchange rate of azurin (28, 29) and the larger width of the paramagnetic signals, compared with amicyanin, prevent the observation of exchange peaks for signals **A** and **C**.

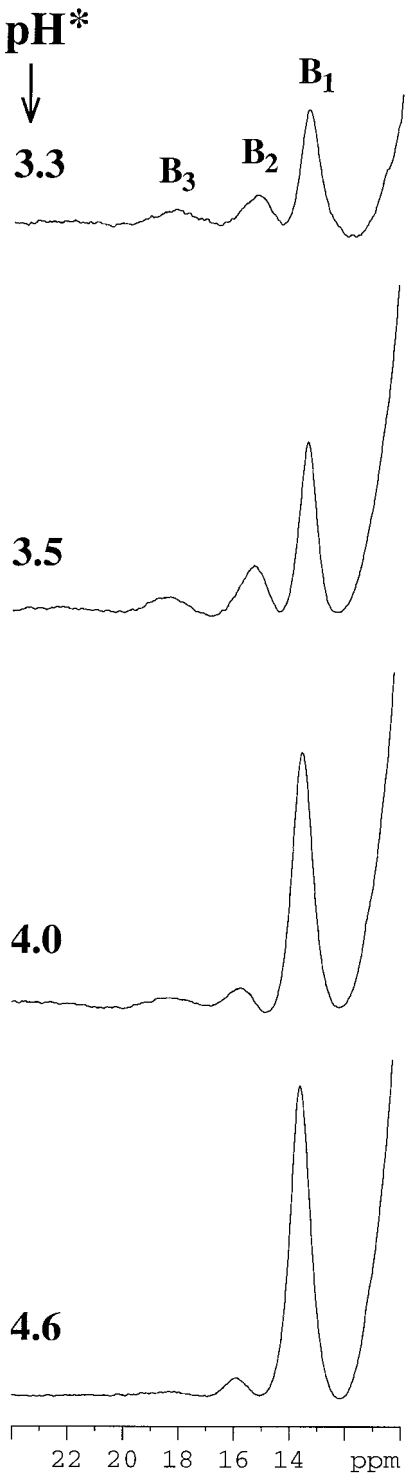

FIG. 3. **Parts of the ^{1}H NMR spectra of Cu(II)-M121H azurin in D_2O at different pH* values and 20 °C.** Notice that the signal-to-noise ratio decreases at the lowest pH* values due to some protein denaturation.

When we compare the spectra of Cu(II)-wt (Fig. 1*A*) and Cu(II)-M121H (Fig. 1*B*) azurins the main differences are the significant sharpening of signal **B** and the presence of two additional small peaks (**2** and **3**) close to this signal in the spectrum of the mutant. We will refer to these peaks as signals $\mathbf{B_2}$ and $\mathbf{B_3}$, and to the main peak **B** as signal $\mathbf{B_1}$ (Fig. 1*B*). Despite the larger width of signal **B** in the wt azurin, the longitudinal relaxation times of this proton are similar for both proteins (T_1 = 9.4 ± 0.3 ms for signal **B** from the wt azurin and

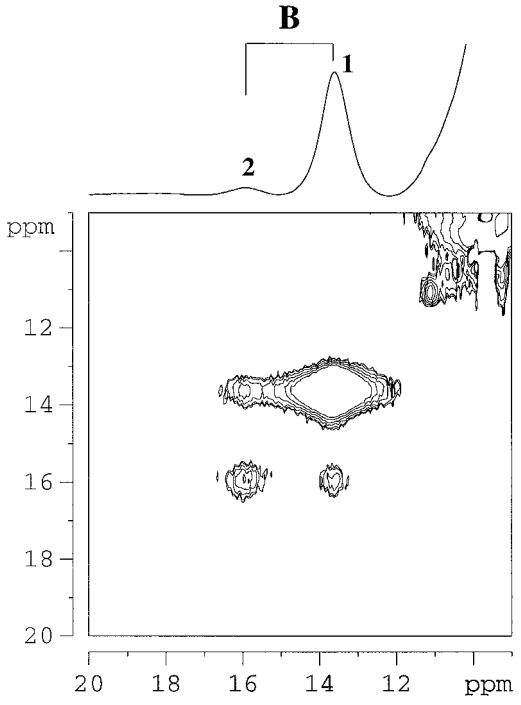

FIG. 4. **WEFT-EXSY spectrum of Cu(II)-M121H azurin (3-ms mixing time) recorded in D_2O at pH* 6.0 and 20 °C.**

8.4 ± 0.2 ms and 7.2 ± 0.5 ms for signals $\mathbf{B_1}$ and $\mathbf{B_2}$ from the M121H azurin, respectively).

No EXSY peaks were observed between reduced and oxidized Cu(II)-M121H azurin due to the low rate of the ESE reaction.[3] By analogy with the wt azurin spectrum (Fig. 1*A*), we assign the peak $\mathbf{B_1}$ as deriving from the Cys^{112} C$^{\alpha}$H proton. As we show further on, the peaks $\mathbf{B_1}$ and $\mathbf{B_2}$ are connected to each other by a slow exchange process.

The spectrum of Cu(II)-M121H azurin does not change between pH* 5 and pH* 11, but below pH* 4.5 signal $\mathbf{B_1}$ decreases in intensity, while the area of the small signals $\mathbf{B_2}$ and $\mathbf{B_3}$ increases (Fig. 3). Signals $\mathbf{B_1}$ and $\mathbf{B_2}$ appear to be connected in an EXSY spectrum where an exchange peak between them is clearly observed (Fig. 4).

Co(II)-M121H Azurin

Due to the limited number of paramagnetically shifted resonances observed in the NMR spectrum of Cu(II)-M121H azurin we have studied also the cobalt derivative of this protein. Co(II)-M121H azurin exhibits a UV-visible spectrum which is similar to that of other cobalt-substituted blue copper proteins (22, 30, 31) (Fig. 5). It is dominated by intense ligand-to-metal charge transfer transitions at 304 and 361 nm, as well as *d-d* (ligand field) transitions between ~500 and ~650 nm. Contrary to the case of the copper derivative of this protein (17) the spectrum changes only slightly with pH (data not shown). These changes consist of a small reduction of the intensity of all the bands at pH values lower than 5 and are not large enough to allow the calculation of a pK_a value.

The ^{1}H NMR spectrum of Co(II)-M121H at pH 6.0 is characterized by a group of paramagnetic signals spread from approximately +220 ppm to −40 ppm (Fig. 6, *A* and *B*). A first inspection of the spectrum already shows that the majority of the paramagnetically shifted signals can be classified into three types, **1**, **2**, and **3**, according to their area (Fig. 6*B*). As explained below, this is due to the existence of three species in

[3] S. Kroes, unpublished observations.

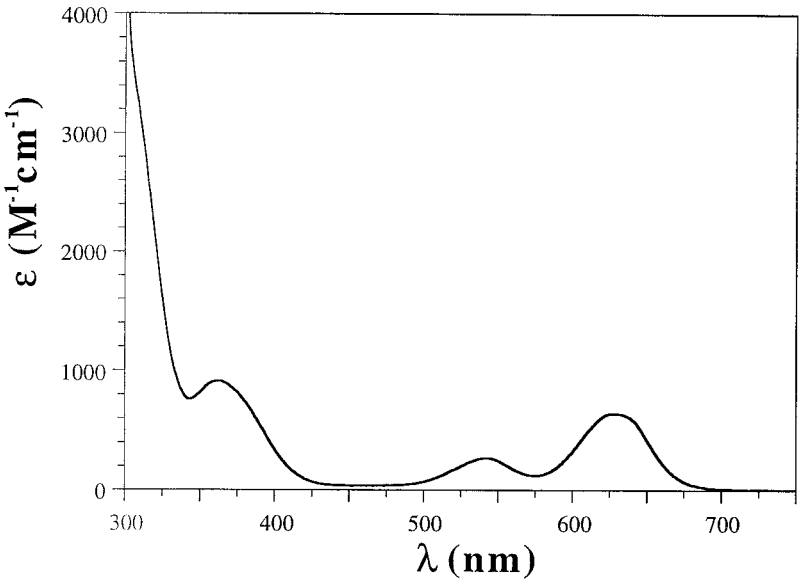

FIG. 5. **UV-Vis spectrum of cobalt(II)-M121H azurin (pH 7, 20 °C).** The molar extinction coefficient values are calculated from the absorption data points using the value of $\epsilon_{280} = 17000\ M^{-1}\ cm^{-1}$ (35). Notice that the ligand-to-metal charge transfer band at ~304 nm appears as a shoulder on the intense UV protein band.

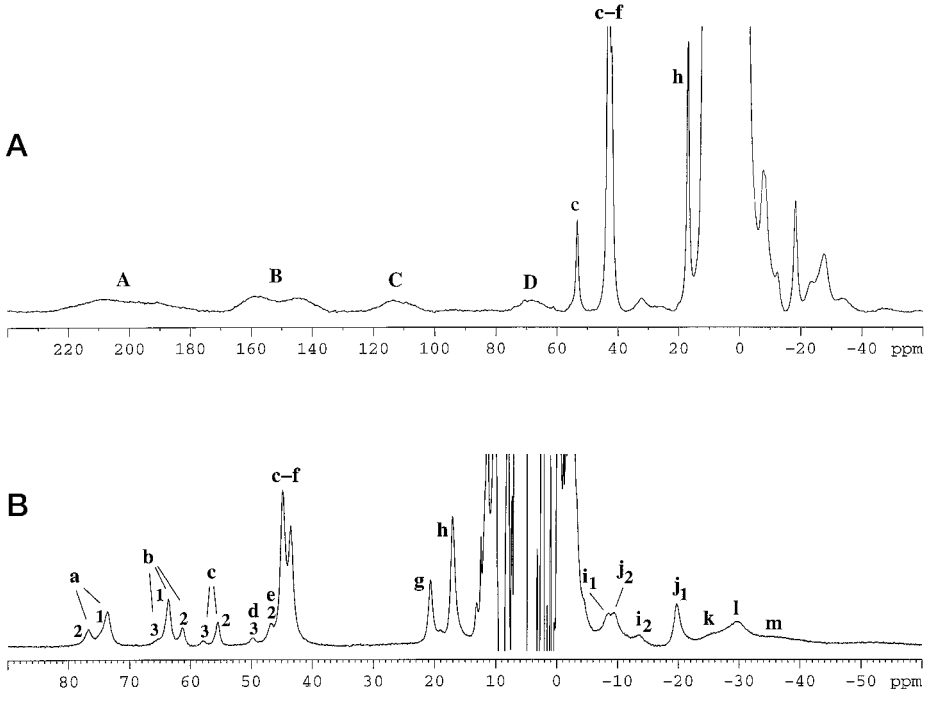

FIG. 6. **^{1}H super-WEFT NMR spectra of Co(II)-M121H azurin at 37 °C (*A*) and 30 °C (*B*).** Signals **a**, **b**, **e**, and **g** are not present in spectrum **A**, recorded in D_2O (pH* 6.0) at 300 MHz. Spectrum **B** has been recorded in H_2O (pH 6.0) at 600 MHz. *Letters* are used to designate different protons, while *numbers* (**1**, **2**, and **3**) refer to the three different species in solution (see the text and Fig. 8).

solution which are in slow exchange. Increasing the temperature changes the equilibrium between these species and the weaker peaks (**3**) disappear (Fig. 7*A*). When the pH is changed from 6.0 to 4.2, only minor variations in signal intensities can be observed (Fig. 7*B*).

In a 4-ms mixing time WEFT-NOESY spectrum recorded at 22 °C and pH 6, exchange cross-peaks are observed which permit grouping together signals that correspond to the same proton (Fig. 8). Although the cross-signals are very clear at these conditions, they are not observed when the temperature or the pH are changed, probably because the exchange rate then becomes too fast or too slow for the EXSY peaks to be observed. This also helps us to discriminate between the exchange cross-peaks and normal NOE cross-peaks, since we do not expect the latter ones to be so strongly dependent on pH and temperature.

In the 30–80 ppm spectral region at least four sets of three signals each can be distinguished, the signals in each set having relative areas of ~5, ~25, and ~70%. The total area of the signals present in this region (**a**–**f**) corresponds to 6 protons, three of which (**a**, **b**, and **e**) are solvent-exchangeable and disappear when the spectrum is registered in D_2O. Ring protons from coordinated histidines in cobalt-substituted proteins are normally hyperfine-shifted into the 30–80 ppm region (32). Thus, all solvent-exchangeable protons found here we ascribe to imidazole NH groups. By analogy with the spectra of the cobalt derivatives of wt azurin and the M121Q mutant (22), as well as with the spectra of other cobalt-substituted blue-copper proteins like Co(II)-stellacyanin (33), the more downfield shifted NH signals (**a** and **b**) are assigned to His^{46} and His^{117}. Of these two, signal **a** disappears at high pH (Fig. 9). The $N^{\epsilon 2}H$ proton of His^{117} is exposed to the solvent and can enter base-catalyzed fast exchange at high pH (34). Thus, signal **a** is assigned to the $N^{\epsilon 2}H$ proton of His^{117}, and the remaining signal (**b**) to the $N^{\epsilon 2}H$ proton of His^{46}. The third group of labile signals (**e**) is overlapping with other (CH) signals at around 44 ppm, and the only resolved signal belonging to this NH group is the small signal at 46.8 ppm, $\mathbf{e_2}$. When the spectrum is recorded in

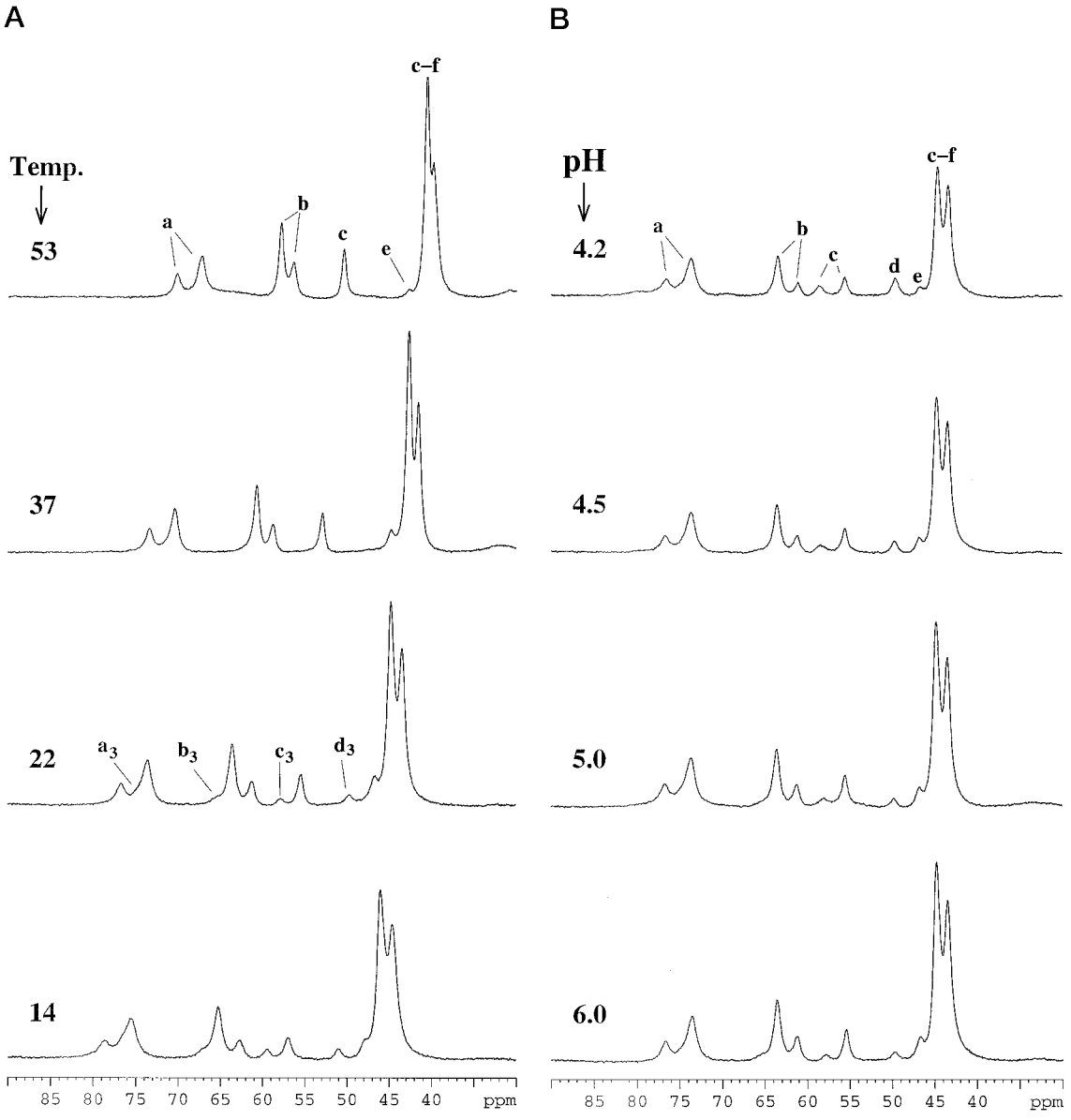

FIG. 7. **Temperature (*A*) and pH (*B*) dependence of the low field region of the ^{1}H NMR spectrum of Co(II)-M121H azurin.** Spectra were recorded at 400 MHz on 4 mM protein samples in H_2O, using a super-WEFT pulse sequence.

D_2O the group of signals between 42 and 48 ppm loses an area corresponding to one proton. We assign these NH signals (**e**) to the His121 $N^{\epsilon 2}H$ proton.

The ring $C^{\delta 2}H$ protons from the coordinated histidines normally give rise to relatively sharp signals in the 30–80 ppm region (21, 22, 32). In the spectrum of the Co(II)-M121H azurin, the signals from the three protons of this type, corresponding to the histidines 46, 117, and 121, overlap between 40–45 ppm (signals designated **c**–**f** in Fig. 6*B*), with the exception of signals $\mathbf{c_2}$ and $\mathbf{c_3}$. NOESY cross-peaks are typically observed between these $C^{\delta 2}H$ signals and the $N^{\epsilon 2}H$ signal of the same histidine ring (21, 22). In the present case, such a correlation peak is only observed between signals $\mathbf{c_1}$ and $\mathbf{b_1}$, (Fig. 8*B*), which allows us to assign signals **c** and **b** to the same histidine (His[46], according to the above assignment of signal **b**).

Other Signals—Although the occurrence and behavior of other paramagnetically shifted signals is less relevant to the main goal of this study we briefly describe them here. The very broad signals corresponding to four protons observed downfield in the NMR spectrum of Co(II)-M121H azurin (Fig. 6*A*, signals **A**–**D**) are a characteristic feature of cobalt-substituted blue copper proteins (21, 22, 25). It has been proven for the wt *P. aeruginosa* azurin that the far downfield shifted signals **A** and **B** correspond to the β protons of Cys[112] (21). With regard to the signals **C** and **D**, similar signals in wt Co(II) and Ni(II) azurin have been tentatively assigned to the ϵ_1 protons of His[46] and His[117] (21, 22), and these assignments have been proven through one-dimensional NOE for a pair of similar signals found in the ^{1}H NMR spectrum of the Ni(II) derivative of the M121Q azurin (22). In the present spectrum these signals appear significantly broader, possibly due to the effect of the exchange process. Moreover, for signals **A** and **B** a splitting into two signals, possibly corresponding to the aforementioned two main species, seems to occur (Fig. 6*A*).

Other paramagnetic signals are observed around 20 ppm (**g** and **h**), as well as in the upfield shifted region between −10 and −40 ppm (**i**–**m**, see Fig. 6*B*). Signal **g** is an exchangeable proton which might correspond to the amide proton of His[117], as a similar signal has been observed for the cobalt derivative of wt *P. aeruginosa* azurin (25). Some of the upfield shifted signals can also be grouped according to the EXSY peaks observed between them (Fig. 8*C*). They could correspond to the β protons

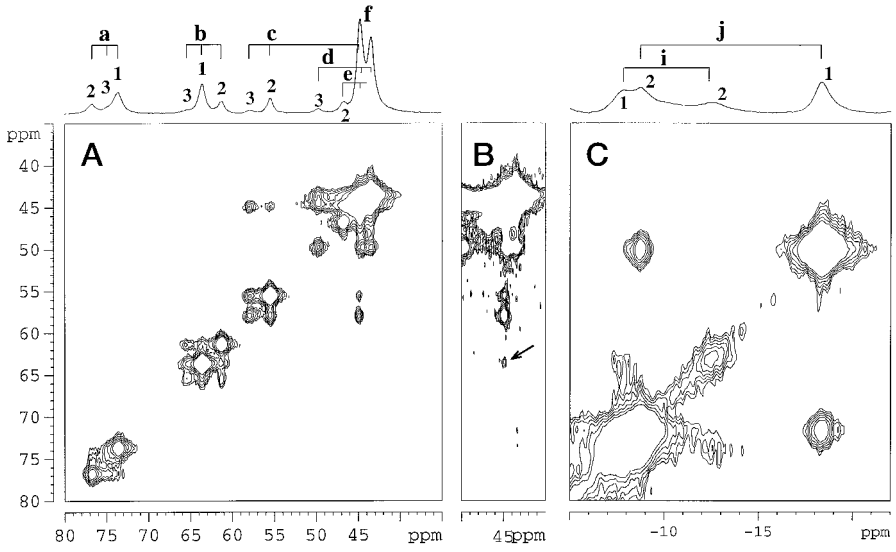

FIG. 8. **Parts of a WEFT-EXSY spectrum (pH 6.0, 22 °C, 4-ms mixing time) of 4 mM Co(II)-M121H azurin.** Exchange cross peaks are observed between species **1**, **2**, and **3** for signals **a**, **b**, **c**, **d**, and **e** (*A*); and between species **1** and **2** for signals **i** and **j** (*C*). *B* shows a different representation of part of the spectrum in *A* where a weak NOESY cross-peak (marked with an *arrow*) can be observed.

of the coordinated histidines, and to residues close to the metal but not bound to it (pseudocontact shifted signals).

High pH Effects—When the pH is increased above 7.5, signal **a**, corresponding to the His^{117} $N^{\epsilon 2}H$ proton, disappears (Fig. 9). As explained before, this is interpreted as being due to a base-catalyzed increase of the exchange rate of this exposed proton (34). Above pH 9.0, new signals appear, while the area of the group of overlapping signals around 44 ppm diminishes. Attempts to correlate these new signals with other ones through EXSY and saturation transfer experiments failed, which indicates that the equilibrium process in which the high pH species participates is very slow.

DISCUSSION

M121H versus Wild Type Azurin, Coordination Geometry in the M121H Azurin

Cu(II) Derivative—In Fig. 1, the ^1H NMR spectrum of Cu(II)-M121H azurin is compared with the corresponding spectrum of Cu(II)-wt azurin from *A. denitrificans*. The main differences are the significant sharpening of signals **B**, a larger shift of signal **C**, and a smaller shift of the signal **B**, in the M121H azurin spectrum. The properties of signal **B**, assigned to the Cys^{112} α proton, can be used as a diagnostic tool to monitor the properties of the metal site, as a strong Cu(II)-S^{γ}(Cys) interaction is considered characteristic of the blue copper proteins. The smaller contact shift of signal **B** observed for the M121H mutant is an indication of a weaker copper-sulfur interaction. This is in agreement with the idea that the metal site in Cu(II)-M121H azurin is more tetrahedral than in the wt azurin and that the metal ion is out of the $N^{\delta}(His^{46})$-$N^{\delta}(His^{117})$-$S^{\gamma}(Cys^{112})$ equatorial plane, since that reduces the copper-sulfur orbital overlap. It is important to notice that there is also a significant difference in the isotropic shifts of the three signals **B** from Cu(II)-M121H, namely $\delta_{B3} > \delta_{B2} > \delta_{B1}$. Thus, the tetrahedral character of species **1**, **2**, and **3** would follow the order: **1** > **2** > **3**, with species **2** and **3** being more similar to wt azurin than species **1**.

The difference in the line-widths of signals **B** from wt and M121H azurin contrasts with their rather similar longitudinal relaxation times. This can be rationalized by invoking the larger contact coupling in wt azurin, since the transverse relaxation is more affected by the contact contribution than the longitudinal relaxation (23).

Co(II) Derivative—Comparing the ^1H NMR spectra of the cobalt derivatives of the wt and M121H azurins we find important differences (for the spectrum of the Co(II)-wt azurin from *A. denitrificans*, see Salgado *et al*. (22)). First, the more downfield shifted resonances (**A** and **B**), typically assigned to the β protons of the coordinated Cys^{112} (21, 22), are much more shifted in the wt protein. This is also found for the Co(II)-M121Q azurin (22) as well as for Co(II)-stellacyanin (33), where it has been connected with a more tetrahedral metal site resulting in a weaker Co(II)-S^{γ}(Cys) interaction. The same interpretation applies in the case of Co(II)-M121H azurin, in good agreement with the above conclusions for the Cu(II) derivative of this protein.

Second, the typical ^1H NMR pattern found for $-CH_2$ groups from ligands in axial positions (the $-C^{\gamma}H_2$ of Met^{121} and the $-C^{\alpha}H_2$ of Gly^{45}) in wt Co(II)-azurins, where one proton is shifted upfield and the other downfield (21, 22), is not found here. In the case of residue 121 this is to be expected as a consequence of the substitution of Met by His, but for the Gly^{45}, these findings indicate that this residue is not coordinated to the metal as in the cobalt-substituted wt azurin.

The differences in the isotropic shifts of the three species observed in the spectrum of the Co(II)-M121H azurin cannot be used directly to infer the precise nature of the coordination geometry of the corresponding species. In Co(II) complexes, in contrast to the Cu(II) complexes, the paramagnetic shifts may contain a significant pseudocontact contribution of which the magnitude is not always easy to establish (23). This is particularly true for distorted tetrahedral and trigonal pyramidal cobalt complexes, which are those normally found in cobalt-substituted blue copper proteins (21, 22).

The Exchange Equilibrium in M121H Azurin

The UV-visible, RR, and EPR spectra of Cu(II)-M121H azurin have been interpreted before by assuming the existence of a simple two site equilibrium (17). Now we find that the situation is in fact more complex and three species can be observed (as illustrated by the occurrence of the peaks $\mathbf{B_1}$, $\mathbf{B_2}$, and $\mathbf{B_3}$, all three corresponding to the $C^{\alpha}H$ proton of Cys^{112}). No proof for a third species was found with other spectroscopic techniques (EPR and UV-visible spectroscopy) (17), most likely because its concentration was below the detection limit. Although no EXSY connection has been established in the NMR spectrum of Cu(II)-M121H azurin between the small signal $\mathbf{B_3}$ and signals $\mathbf{B_1}$ and $\mathbf{B_2}$, the fact that such a connection is clearly observed for the three species of the Co(II)-M121H azurin supports the existence of an equilibrium between three species also in Cu(II)-M121H. Further proof for this conclusion comes from

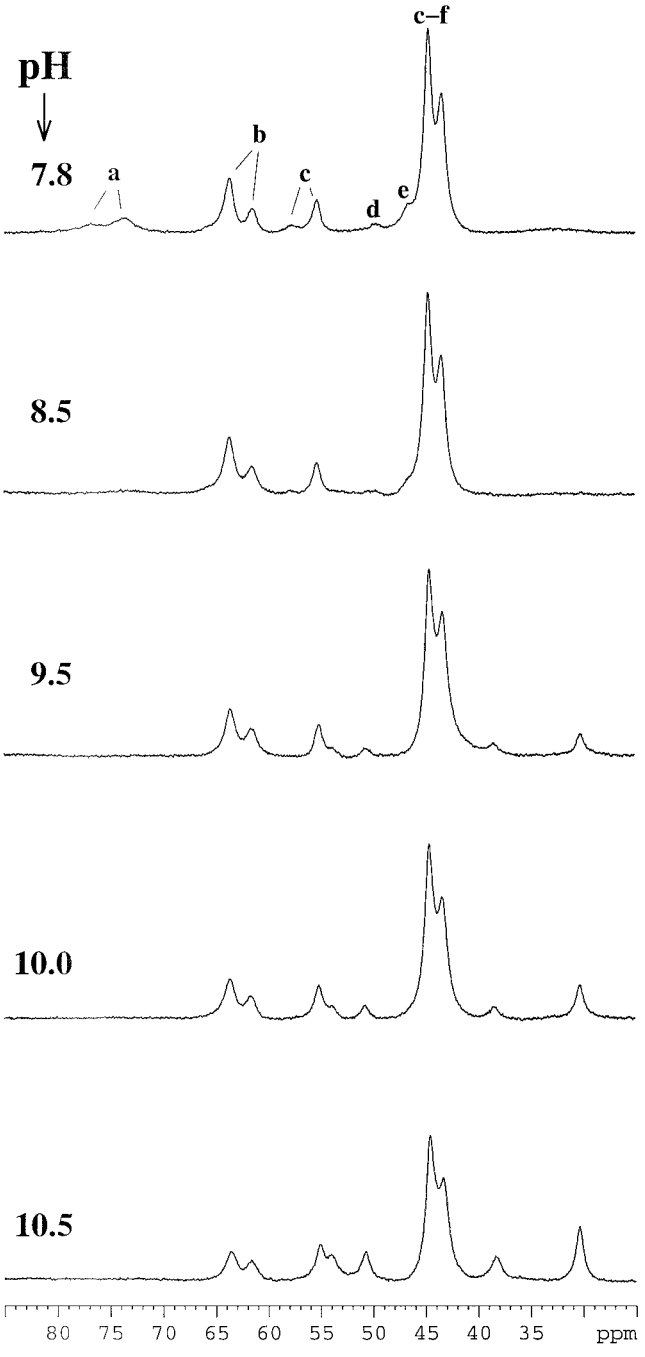

FIG. 9. **1H NMR spectra of Co(II)-M121H azurin (22 °C) at pH values ranging from 7.8 to 10.5.** Spectra were recorded at 400 MHz on 4 mM protein samples in H_2O, using a super-WEFT pulse sequence.

the analysis of the pH behavior of peaks $\mathbf{B_1}$, $\mathbf{B_2}$, and $\mathbf{B_3}$ (see below).

The area of the ^{1}H NMR signals corresponding to the three species in the Cu(II) derivative indicate that they are present at relative concentrations of ~1, ~5, and ~94%. Assuming that the two main species observed here by NMR are the ones characterized previously by Uv-visible, RR, and EPR (17), we conclude that the more intense signal in the ^{1}H NMR spectrum (**1**) corresponds to a type 1.5 copper site while signals **2** and **3** correspond to type 1 copper sites. The fact that the latter signals present larger isotropic shifts (see above) is in agreement with their assignment to type 1 species.

Now that the concentrations of the various species in solution have been be established, the extinction coefficients of the optical bands of the type 1.5 site can be quantitated. By using the wild type values for the extinction coefficients for the type 1 site ($\epsilon_{280} = 2.7 \times 10^4$ M^{-1} cm^{-1}, $\epsilon_{619} = 5.1 \times 10^3$ M^{-1} cm^{-1}) (24, 35) the corresponding coefficients for the type 1.5 site are determined as $\epsilon_{439} = 2.7 \times 10^3$ M^{-1} cm^{-1} and $\epsilon_{593} = 1.2 \times 10^3$ M^{-1} cm^{-1} from the optical data at pH 7 at room temperature. Additionally, from the NMR data an approximate value of 1 ms can be estimated for the time scale on which the interconversion of the various species occurs at room temperature.

Also in the case of Co(II)-M121H azurin, the presence of three signals for every proton in the ^{1}H NMR spectra is an indication of the existence of three different species in solution which interconvert slowly on the NMR time scale. From the relative area of the signals it is concluded that the dominant species represents about 70% of the total amount of Co(II)-M121H in solution, while the other two represent approximately 25 and 5%. These proportions vary slightly with temperature and pH. Thus, the two main species (**1** and **2**) are present at any pH ($4.2 < \text{pH} < 10.5$) or temperature ($14\ °C < T < 53\ °C$), but the minor (**3**) species is only observed below 30 °C and increases slightly in intensity at low pH. Despite similar NMR observations on the Cu(II)- and Co(II)-M121H azurins, the ratio between the three observed species is different for the two metalloderivatives, compatible with slightly different coordination geometries.

The occurrence of more than one species is related to the position of the copper with regard to the equatorial plane formed by the $N^{\delta}46$, $N^{\delta}117$, and $S^{\gamma}112$ ligands and to the axially located groups, the $N^{\delta}121$ and the Gly^{45} carbonyl. In species **1** the metal has moved out of the equatorial plane toward the His^{121} N^{δ}, giving rise to a type 1.5 site (17), while species **2** and **3** correspond to configurations in which the Cu(II)-$N^{\delta}(His^{121})$ bond has been elongated and the metal has moved back to the equatorial plane in the direction of the Gly^{45} oxygen. Moreover, an additional ligand (H_2O or OH^-) may come into play (17–19) when species **1** transforms into species **2** and **3**. A qualitative illustration is presented in Fig. 10.

It is noted that in the EXSY spectrum of Co(II)-M121H azurin the exchange peaks between signals **3** and **1** and between signals **3** and **2** are stronger than those between signals **2** and **1**, despite the low intensity of signal **3** (Fig. 8*A*). This is a strong indication that, in the exchange path between species **1** and **2**, species **3** is an intermediate. As discussed before, the larger shift of signal $\mathbf{B_3}$ in the spectrum of Cu(II)-M121H azurin also suggests that the metal is located closer to the equatorial plane at a position intermediate between the His^{121} N^{δ} and the Gly^{45} oxygen. When representing the exchange process by a single reaction coordinate, the three species **1–3** correspond with potential energy minima of different depths (Fig. 10). As is known from NMR and x-ray crystallography data, Zn(II) (36), Ni(II) (22, 37), and Co(II) (21, 22) in metallo-substituted wt azurins differ from Cu(II) (13) in their preference to move in the direction of the carbonyl oxygen of Gly^{45} away from residue Met^{121}. One expects, therefore, potential energy wells **2** and **3** in Fig. 10 to be less shallow for the Cu(II)-M121H azurin than for the Co(II)-M121H azurin, in agreement with the observation of a larger population of species **2** and **3** in the latter.

The pH Effect

When the pH is lowered, signals $\mathbf{B_2}$ and $\mathbf{B_3}$ of the spectrum of Cu(II)-M121H azurin gain intensity at the expense of signal $\mathbf{B_1}$ (Fig. 3). Although the titration curve could not be completed, due to the instability of the protein at low pH, the data can be fit by using Equation 1 assuming a single equilibrium (Fig. 11), from which a $pK_a^{ap} = 3.1 \pm 0.2$ was obtained. The value of this

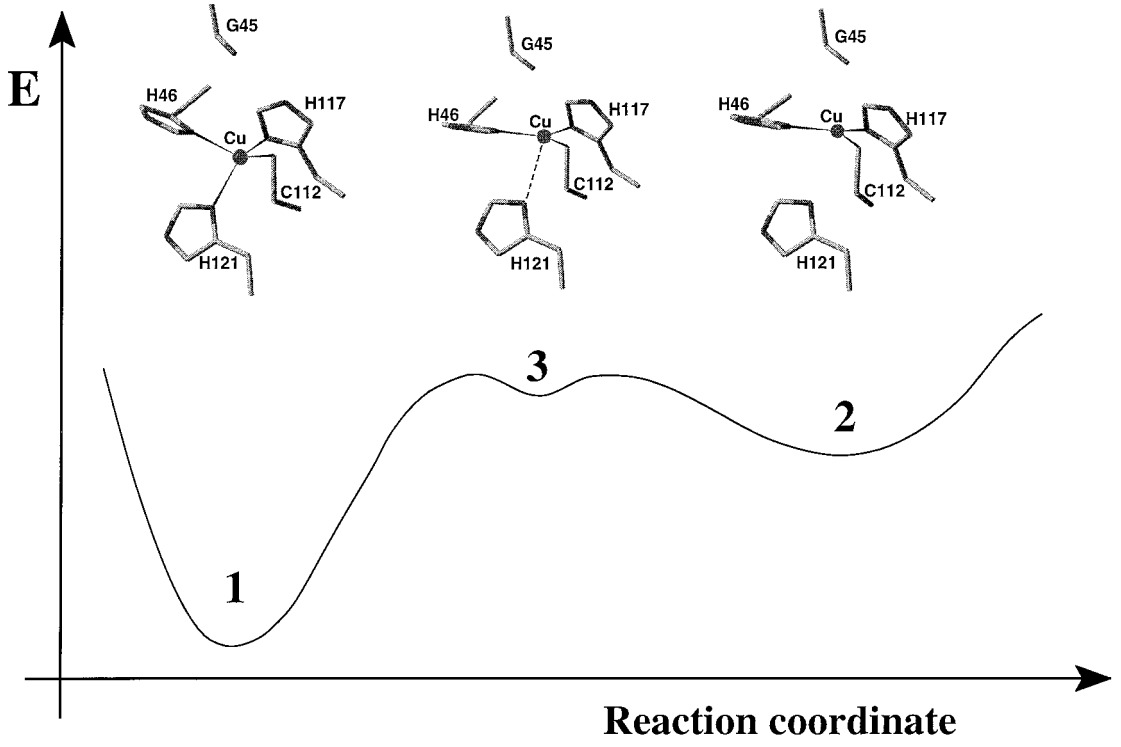

FIG. 10. **Schematic representation of the potential energy, *E*, of the copper site in M121H azurin as a function of the displacement of the metal along the axial coordinate *Q*.** On *top* are schematic representations of the three species found in solution. Species **1** is based on x-ray diffraction data obtained on M121H azurin at pH 6.5 (A. Messerschmidt, unpublished observation). Species **2** and **3** have been modeled according to the present NMR results and evidence from UV-visible, RR, EPR, and perturbed angular correlation spectroscopy (17, 19). In species **2** and **3** an additional ligand (not shown) may be present (18, 19).

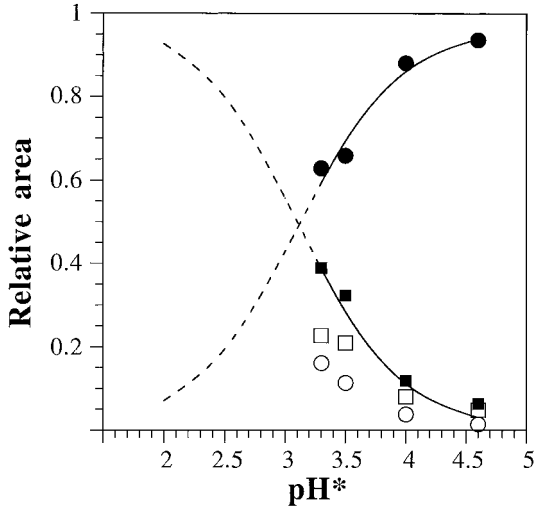

FIG. 11. **Plot of the relative area of signals B_1, (*filled circles*) B_2 (*open squares*), B_3 (*open circles*), and $B_2 + B_3$ (*filled squares*) from the ^{1}H NMR spectra of Cu(II)-M121H azurin (Fig. 3) *versus* pH*.** Fitting of the data has been performed by using Equation 1.

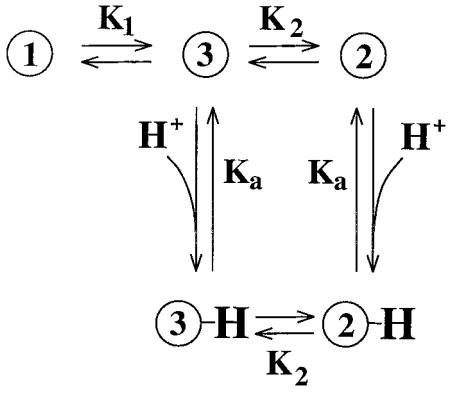

SCHEME 1.

"apparent" pK_a can be interpreted by considering the equilibria between the species **1**, **2**, and **3** present in solution. As the pH effect has been connected with the ionization of His^{121} (17), it is reasonable to assume that species **2** and **3** protonate according to Scheme 1, where K_a is the (intrinsic) protonation constant of His^{121} in species **2** and **3**. One then finds that

$$pK_a^{ap} = pK_a + \log(K_1 + K_1K_2) \qquad \text{(Eq. 2)}$$

The equilibrium constants K_1 and K_2, defined in Scheme 1, can be calculated from the relative amounts of the species **1**, **2**, and **3** at pH > 5.0 (94, 5, and 1%, respectively, see above). They amount to 0.05 and 0.2, respectively. From Equation 2, and using a pK_a^{ap} = 3.1, a pK_a = 4.3 ± 0.2 is then obtained. The apparent pK_a^{ap} of 3.1 is smaller than the value determined (17) from the optical spectra (3.8). Although the optical titration was performed on solutions in H_2O, while the present data are obtained in D_2O, this is unlikely to be the cause of the difference, since for the present pK_a^{ap} value, determined from non-corrected pH meter readings, the variations of the pK_a (D_2O) are expected to compensate the pH readings variations (38, 39) and fall within the error limits of the experiment. We ascribe the difference between the two pK_a values to experimental uncertainty caused by the instability of the protein below pH 3.5.

Conclusion

Despite the intensive efforts of a number of groups in recent years, the characteristics of a type 1.5 copper site remained elusive. Optically it appeared impossible to distinguish a type 1.5 site (pronounced bands around 450 and 600 nm) from a

mixture of a type 1 site (strong band around 600 nm) and a type 2 site with a cysteinate copper ligand (strong band around 400–450 nm). Similarly, EPR spectroscopy at low temperature appeared insufficiently sensitive and had insufficient resolution to distinguish and accurately quantitate various species in solution. Moreover the switch to the low temperatures at which EPR spectra are usually recorded, may affect the equilibrium between the various species in solution. For similar reasons RR spectroscopy appeared not a suitable technique for quantitation of different species. Without a reliable determination of concentrations it also appeared impossible to analyze the pH dependence of the site.

In the present study it has been shown that NMR of the paramagnetic forms of the type 1.5 site (Cu(II) and Co(II)-substituted) could be used directly to determine the concentrations of the various species in solution. In this way, for the first time the identity and dynamic behavior of the various species co-existing in solution could be established. All the available experimental evidence fit within the proposed Scheme 1. At high pH there are two main species in solution, species 1 representing the type 1.5 site and species 2 corresponding with a "rhombic" type 1 site. The behavior of His^{121} is crucial in this respect. In the type 1.5 site His^{121} binds directly to the copper, pulling the metal out of the N_2S plane of the three ligands; in the type 1 sites the Cu-His^{121} bond is weaker, similar to a Cu-Met^{121} bond, presumably because the histidine has moved away from the copper. From the NMR data it can be concluded, moreover, that the interconversion of the two species takes place through an intermediate form (species 3) which is present at very low concentrations. The low concentration explains why this site has not been observed by other spectroscopic techniques.

At low pH only species 2 and 3 are converted into protonated forms. This explains the initially perplexing observation in which the type-1 optical spectrum observed at low pH, changes into a type 1.5 spectrum at high pH while it appeared impossible to complete the titration. According to Scheme 1 the equilibrium between the deprotonated forms of species 1, 2, and 3 is independent of pH, which is why at high pH the relative concentrations of the three species do not change anymore with pH.

Important lessons from this work that may be of relevance for future attempts at metal site engineering in proteins are: 1) a native metal site may be converted into a new site, which even when stable, may occur in various configurations which interconvert in the millisecond to second time regime; 2) the ligand configurations may differ not only in their conformation, but also with respect to the number of ligands. External ligands (water, hydroxide) may come into play; and 3) a newly created site may become susceptible to pH effects. This may influence the site behavior in a complex manner which may not be evident from the optical properties.

It is conceivable that the activity of the new site is dictated by the time the metal spends in a particular configuration which does not need to be the main species. This can be of particular relevance when optimization of activity is attempted.

Acknowledgments—We acknowledge Dr. A. Messerschmidt for providing us with structural information of Cu(II)-Met121His azurin and Dr. L. Bubacco for helpful discussions.

REFERENCES

1. Hellinga, H. W. (1996) in *Design of Metalloproteins* (Cleland, J. L., and Craik, C. S., eds) pp. 369–398, Wiley-Liss, New York
2. Regan, L. (1993) *Annu. Rev. Biophys. Biomol. Struct.* **22,** 257–281
3. Higaki, J. N., Haymore, B. L., Chen, S., Fletterick, R. J., and Craik, C. S. (1990) *Biochemistry* **29,** 8582–8586
4. Browner, M. F., Hackos, D., and Fletterick, R. (1994) *Nat. Struct. Biol.* **1,** 327–333
5. Stewart, J. D., Roberts, V. A., Crowder, M. W., Getzoff, E. D., and Benkovic, S. J. (1994) *J. Am. Chem. Soc.* **116,** 415–416
6. Pinto, A. L., Hellinga, H. W., and Caradonna, J. P. (1997) *Proc. Natl. Acad. Sci. U. S. A.* **94,** 5562–5567
7. Matthews, D. J. (1995) *Curr. Opin. Biotechnol.* **6,** 419–424
8. Barrick, D. (1995) *Curr. Opin. Biotechnol.* **6,** 411–418
9. Barrick, D. (1994) *Biochemistry* **33,** 6546–6554
10. Lu, Y., LaCroix, L. B., Lowery, M. D., Solomon, E. I., Bender, C. J., Peisach, J., Roe, J. A., Gralla, E. B., and Valentine, J. S. (1993) *J. Am. Chem. Soc.* **115,** 5907–5918
11. Mizoguchi, T. J., Di Bilio, A. J., Gray, H. B., Richards, J. H. (1992) *J. Am. Chem. Soc.* **114,** 10076–10078
12. Canters, G. W., and Gilardi, G. (1993) *FEBS Lett.* **325,** 39–48
13. Baker, E. N. (1988) *J. Mol. Biol.* **203,** 1071–1095
14. Solomon, E. I., and Lowery, M. D. (1993) *Science* **259,** 1575–1581
15. den Blaauwen, T., and Canters, G. W. (1993) *J. Am. Chem. Soc.* **115,** 1121–1129
16. Karlsson, B. G., Nordling, M., Pascher, T., Tsai, L. C., Sjölin, L., and Lundberg, L. G. (1991) *Protein Eng.* **4,** 343–349
17. Kroes, S. J., Hoitink, C. W. G., Andrew, C. R., Ai, J., Sanders-Loehr, J., Messerschmidt, A., Hagen, W. R., and Canters, G. W. (1996) *Eur. J. Biochem.* **240,** 342–351
18. Kroes, S. J., Salgado, J., Parigi, G., Luchinat, C., and Canters, G. W. (1996) *J. Biol. Inorg. Chem.* **1,** 551–559
19. Danielsen, E., Kroes, S. J., Canters, G. W., Bauer, R., Hemmingsen, L., Singh, K., and Messerschmidt, A. (1997) *Eur. J. Biochem.*, in press
20. Kalverda, A. P., Salgado, J., Dennison, C., and Canters, G. W. (1996) *Biochemistry* **35,** 3085–3092
21. Piccioli, M., Luchinat, C., Mizoguchi, T. J., Ramírez, B. E., Gray, H. B., and Richards, J. H. (1995) *Inorg. Chem.* **34,** 737–742
22. Salgado, J., Jiménez, H., Moratal, J. M., Kroes, S., Warmerdam, G., and Canters, G. W. (1996) *Biochemistry* **35,** 1810–1819
23. Bertini, I., and Luchinat, C. (1986) *NMR of Paramagnetic Molecules in Biological Systems*, Benjamin/Cummings Publishing Co., Menlo Park, CA
24. Hoitink, C. W. G., and Canters, G. W. (1992) *J. Biol. Chem.* **267,** 13836–13842
25. Salgado, J., Jiménez H. R., Donaire, A., and Moratal, J. M. (1995) *Eur. J. Biochem.* **231,** 358–369
26. Inubushi, T., and Becker, E. D. (1983) *J. Magn. Reson.* **51,** 128–133
27. Chen, Z., de Ropp, J. S., Hernández, G., and La Mar, G. N. (1994) *J. Am. Chem. Soc.* **116,** 8772–8783
28. Groeneveld, C. M., Ouwerling, M. C., Erkelens, C., and Canters, G. W. (1988) *J. Mol. Biol.* **200,** 189–199
29. Lommen, A., and Canters, G. W. (1990) *J. Biol. Chem.* **265,** 2768–2774
30. McMillin, D. R., Rosenberg, R. C., and Gray, H. B. (1974) *Proc. Natl. Acad. Sci. U. S. A.* **71,** 4760–4762
31. Di Bilio, A. J., Chang, T. K., Malmström, B. G., Gray, H. B., Karlsson, B. G., Nordling, M., Pascher, T., and Lundberg, L. G. (1992) *Inorg. Chim. Acta* **198–200,** 145–148
32. Bertini, I., Turano, P., and Vila, A. (1993) *Chem. Rev.* **93,** 2833–2932
33. Vila, A. J. (1994) *FEBS Lett.* **355,** 15–18
34. Moratal, J. M., Salgado, J., Donaire, A., Jiménez, H. R., and Castells, J. (1993) *Inorg. Chem.* **32,** 3587–3588
35. Hoitink, C. W. G. (1993) *Engineering of the Copper Site of Azurin from Alcaligenes Denitrificans*, Ph.D. thesis, University of Leiden
36. Nar, H., Huber, R., Messerschmidt, A., Filippou, A. C., Barth, M., Jaquinod, M., van de Kamp, M., and Canters, G. W. (1992) *Eur. J. Biochem.* **205,** 1123–1129
37. Moratal, J. M., Romero, A., Salgado, J., Perales-Alarcón, A., and Jiménez, H. R. (1995) *Eur. J. Biochem.* **228,** 653–657
38. Covington, A. K., Paabo, M., Robinson, R. A., and Bates, R. G. (1968) *Anal. Chem.* **40,** 700–701
39. Robinson, R. A., Paabo, M., and Bates, R. G. (1969) *J. Res. Natl. Bur. Stand.-A* **73,** 299–302

The Dynamic Properties of the M121H Azurin Metal Site as Studied by NMR of the Paramagnetic Cu(II) and Co(II) Metalloderivatives

Jesús Salgado, Sandra J. Kroes, Axel Berg, José M. Moratal and Gerard W. Canters

J. Biol. Chem. 1998, 273:177-185.
doi: 10.1074/jbc.273.1.177